

## Ru-Fe<sub>3</sub>O<sub>4</sub>-Containing Polymeric Catalysts for Cellulose Hydrogenolysis

Oleg V. Manaenkov\*, Olga V. Kislitsa, Ekaterina A. Ratkevich, Valentina G. Matveeva, Mikhail G. Sulman, Esther M. Sulman

Tver State Technical University, Department of Biotechnology and Chemistry, 22, Af. Nikitina St., 170026, Tver, Russia  
 ovman@yandex.ru

In this paper, a novel catalysts on the base of hypercrosslinked polystyrene (HPS) with magnetic properties are proposed for the one-pot processes of the cellulose conversion into ethylene glycol (EG) and propylene glycol (PG). Synthesized magnetically recoverable supports and catalysts were characterized by different physical-chemical methods. The magnetic properties of the supports Fe<sub>3</sub>O<sub>4</sub>/HPS MN270 and the corresponding catalysts were studied. The use of this catalyst in the process of microcrystalline cellulose hydrogenolysis in subcritical water allows PG and EG selectivities of 20.0 and 22.6%, respectively, at 100% of cellulose conversion.

### 1. Introduction

Glycols are an important feedstock; they are commonly used in different branches of modern industry. Ethylene glycol and propylene glycol are used in manufacturing medicines, fuels, surfactants, antifreeze, lubricants, and solvents (Yue et al., 2012). Propylene glycol is also used for the synthesis of lactic acid, which is used in the production of biodegradable polylactones (Sugiyama et al., 2013).

It is obvious that the demand for these polyols is extremely high. In addition, the present-day production of EG and PG is based on the use of non-renewable petroleum feedstocks. The development of new efficient methods for the production of these polyols from renewable raw materials is therefore of great interest. EG and PG can thus be obtained via cellulose hydrogenolysis in subcritical water in the presence of heterogeneous catalysts (Luo et al., 2007).

Analysis of current publications shows that in recent years processes with the use of reusable catalysts have been one of the most interesting and relevant topics in chemistry, both in the academic field and in the industry (Wang and Astruc, 2014<sup>a</sup>). New possibilities in catalysis are offered by the use of magnetically recoverable catalysts. Magnetically recoverable Ru-containing catalysts have so far found application in olefin exchange, azide-alkyne cycloaddition, oxidation, hydrolysis, hydrogenation, and other reactions (Wang and Astruc, 2014<sup>b</sup>). Magnetically recoverable catalysts have shown good results in processes of cellulose conversion (Podolean et al., 2014). In (Zhang et al., 2014) in particular, the direct conversion of cellulose to sorbitol was conducted in the presence of a Ni<sub>4.63</sub>Cu<sub>1</sub>Al<sub>1.82</sub>Fe<sub>0.79</sub> catalyst. At a temperature 215 °C, hydrogen partial pressure 4 MPa and the duration of the process 3 hours sorbitol yield was 68.07 %. The catalyst showed high activity after being used three, four times.

In this research, a new catalytic system with magnetic properties, based on the mesoporous matrix of hypercrosslinked polystyrene (HPS) was developed. Hypercrosslinked polymeric materials are promising organic carriers for the synthesis of nanoparticles of controlled-size metals, their stabilization and subsequent use in catalysis (Sidorov et al., 1999). Rigid hypercrosslinked polymers have a very large internal surface, usually about 1000 m<sup>2</sup>/g, and also the ability to swell in any liquid medium, including precipitates for the starting polymer (Tsvetkova et al., 2012). Ru-Fe<sub>3</sub>O<sub>4</sub>-containing catalyst based on HPS MN270 particles exhibiting magnetic properties is proposed for the hydrogenolysis of cellulose to glycols.

## 2. Experimental

### 2.1 Materials

HPS Macronet MN270 (Purolite Int., United Kingdom) was washed with distilled water and acetone and dried under vacuum. Tetrahydrofuran (THF,  $\geq 99.9\%$ ), ethanol (EtOH,  $\geq 99.8\%$ ), methanol (MeOH, 99.5%), sodium hydroxide (NaOH,  $\geq 98\%$ ), iron (III) chloride ( $\text{FeCl}_3$ , 97%) and sodium acetate ( $\text{CH}_3\text{COONa}$   $\geq 99\%$ ) were obtained from Sigma-Aldrich. Ruthenium (IV) hydroxochloride (pure, OJSC Aurat, Russia) was used as received. All chemicals were used as received. Distilled water was purified with an Elsi-Aqua water purification system.

### 2.2 The catalyst 3 % Ru- $\text{Fe}_3\text{O}_4$ /HPS MN270 synthesis

HPS-based magnetically recoverable Ru-containing catalysts were synthesized according to the following procedure. First,  $\text{Fe}_3\text{O}_4$  particles were formed in the polymeric matrix of HPS. In a typical experiment, 0.3 g of HPS of MN270 type with sizes of granules less than 45  $\mu\text{m}$  was placed to the 10 mL of EtOH with preliminarily dissolved calculated amounts of  $\text{FeCl}_3$  and  $\text{CH}_3\text{COONa}$ . After vigorous stirring, the sample of iron-containing HPS was dried at 70  $^\circ\text{C}$ , wetted with ethylene glycol and placed in an autoclave reactor with Teflon coating. Then, the sample was heated up to 200  $^\circ\text{C}$  in argon medium and maintained at this temperature for 5 h. Resulting  $\text{Fe}_3\text{O}_4$ /HPS was washed with distilled water several times and then with EtOH while being maintained by a rare-earth magnet. Washed sample of magnetically separable  $\text{Fe}_3\text{O}_4$ /HPS containing ca. 20 wt. % of Fe was dried at 70  $^\circ\text{C}$  till constant weight was achieved.

For the synthesis of Ru- $\text{Fe}_3\text{O}_4$ /HPS catalyst,  $\text{Fe}_3\text{O}_4$ /HPS MN270 was impregnated according to moisture absorption capacity with the solution of the calculated amount of ruthenium (IV) hydroxochloride in a complex solvent consisting of tetrahydrofuran, methanol, and water at a volume ratio 4:1:1 at room temperature. Further, the catalyst was dried at 70  $^\circ\text{C}$ , consecutively treated with solutions of NaOH and  $\text{H}_2\text{O}_2$ , and then washed with water until the absence of chloride anions in the washing water. The catalyst purified was dried at 85  $^\circ\text{C}$ . Then the catalyst was reduced in hydrogen flow (flow rate 100 mL/min) at 300  $^\circ\text{C}$  for 2 hours, cooled in nitrogen and kept under air. In this way, Ru-containing system with calculated ruthenium content of 3 wt.% was synthesized.

### 2.3 Characterization

Electron-transparent specimens for transmission electron microscopy (TEM) were prepared by placing a drop of a sample suspension onto a carbon-coated Cu grid. Images were acquired at an accelerating voltage of 80 kV on a JEOL JEM1010 transmission electron microscope. Images were analyzed with the National Institute of Health developed image-processing package ImageJ (NIH) to estimate nanoparticle diameters.

X-ray powder diffraction (XRD) patterns were collected on an Epyrean from PANalytical. X-rays were generated from a copper target with a scattering wavelength of 1.54  $\text{\AA}$ . The step-size of the experiment was 0.02. Magnetic measurements were performed on a vibration magnetometer VIBRACH (TvSU, Russia).

X-ray photoelectron spectroscopy (XPS) experiments were performed using PHI Versa Probe II instrument equipped with a monochromatic Al K(alpha) source. The X-ray power of 25 W at 15 kV was used for a 100  $\mu\text{m}$  beam size. Nitrogen adsorption measurements were carried out at liquid nitrogen temperature on a surface analyzer Beckman Coulter SA 3100 (Coulter Corporation, USA). Samples were degassed at 90  $^\circ\text{C}$  in vacuum. X-ray fluorescence (XRF) measurements to determine the Ru and Fe content were performed with a Zeiss Jena VRA-30 spectrometer (Mo anode, LiF crystal analyzer, and SZ detector). Analyses were based on the Co  $K\alpha$  line and a series of standards prepared by mixing 1 g of polystyrene with 10-20 mg of standard compounds. The time of data acquisition was constant at 10 s.

### 2.4 Catalyst testing procedure and product analysis

Our tests were conducted in a 50-cm<sup>3</sup> high-pressure steel reactor (Parr Instruments, USA) equipped with a PARR 4843 controller and a propeller stirrer. In a typical test, the cellulose, the catalyst, and 30 mL of distilled water were placed into the reactor. The reactor was triply purged with hydrogen at a pressure of 60 bar; heating and stirring ( $\approx 100$  rpm). Upon reaching the operational temperature, the speed of the stirrer was increased to 600 rpm. This time was considered to be the starting point of the test. After each test, the catalyst was separated using a neodymium magnet. The liquid phase of the catalyst was analyzed on an UltiMate 3000 liquid chromatograph (Dionex, USA) equipped with a refractometric detector. Cellulose conversion was calculated using the formula  $X = [(m_{c0} - m_c)/m_{c0}] \times 100\%$ , where  $m_c$  is the weight of the cellulose residue after the reaction and  $m_{c0}$  is the initial weight of the cellulose. Selectivity was calculated with the formula  $S = [m_{pr}/(m_{c0} - m_c)] \times 100\%$ , where  $m_{pr}$  is the weight of the respective product.

### 3. Results and discussions

#### 3.1 Characterization

The magnetic properties of the synthesized Fe<sub>3</sub>O<sub>4</sub>/HPS MN270 samples were studied. The magnetization curves are presented in Figure 1. The experimental samples were shown to have a high saturation magnetization ( $4.0 \pm 0.5$  emu/g, Figure 1). This value is significantly higher than the value obtained for the Fe<sub>3</sub>O<sub>4</sub>-SiO<sub>2</sub> synthesized in our previous studies – 0.8 emu/g (Manaenkov et al., 2016<sup>a</sup>, 2016<sup>b</sup>). The magnetization curves no remanence or coercivity is observed, demonstrating superparamagnetic behavior which is characterized for magnetite. A high value of saturation magnetization allows for fast magnetic separation of the Fe<sub>3</sub>O<sub>4</sub>/HPS MN270 particles (Figure 2).

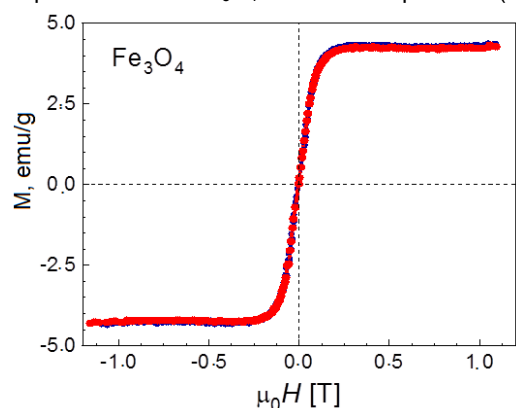


Figure 1: Magnetic properties of Fe<sub>3</sub>O<sub>4</sub>/HPS MN270.

Figure 2: Fe<sub>3</sub>O<sub>4</sub>/HPS MN270 before and after magnetic separation.

In Table 1 the results of X-ray fluorescence measurements are presented. From the data presented, it can be seen that the catalyst synthesis procedure provides final ruthenium content in the catalyst close to the Ru loading (3 %). The average iron content is 19.6 %. Table 2 shows the porosity data of the initial HPS MN 270 and Fe<sub>3</sub>O<sub>4</sub>/HPS MN270 samples and the catalysts obtained from the nitrogen physisorption measurements.

Table 1: The results of X-ray fluorescence measurements

Sample:	%wt.	
	Fe	Ru
Fe <sub>3</sub> O <sub>4</sub> /HPS MN270	19.6	-
3 % Ru-Fe <sub>3</sub> O <sub>4</sub> /HPS MN270	19.6	2.7

Table 2: Porosity data for the initial HPS MN270, Fe<sub>3</sub>O<sub>4</sub>/HPS MN270 and the catalyst 3 % Ru-Fe<sub>3</sub>O<sub>4</sub>/HPS MN270

Sample	BET		Langmuir		t-plot		
	S <sub>BET</sub> , m <sup>2</sup> /g	k <sub>BET</sub>	S <sub>L</sub> , m <sup>2</sup> /g	k <sub>L</sub>	S <sub>t</sub> , m <sup>2</sup> /g	k <sub>t</sub>	V, cm <sup>3</sup> /g
HPS MN270	1075	0.99964	1191	0.9996	265 <sup>1)</sup> ; 807 <sup>2)</sup> ; 1072	0.99816	0.37
Fe <sub>3</sub> O <sub>4</sub> /HPS MN270	450	0.99976	480	0.9992	160 <sup>1)</sup> ; 289 <sup>2)</sup> ; 449	0.99902	0.13
3 % Ru-Fe <sub>3</sub> O <sub>4</sub> /HPS MN270	364	0.99982	392	0.9990	175 <sup>1)</sup> ; 189 <sup>2)</sup> ; 364	0.99968	0.08

S<sub>L</sub> is the specific surface area (Langmuir model); S<sub>BET</sub> is the specific surface area (BET model); S<sub>t</sub> is the specific surface area (t-plot); k<sub>L</sub>, k<sub>BET</sub>, k<sub>t</sub> are the correlation coefficients; <sup>1)</sup> specific surface area according to t-plot model; <sup>2)</sup> specific surface area of micropores; V is the micropores volume.

It was shown that with the successful introduction of iron oxide and ruthenium into the pores of the support, the specific surface area is expected to decrease from 1075 to 364 m<sup>2</sup>/g (BET). The volume of micropores decreases from 0.37 to 0.08 m<sup>3</sup>/g. At the same time, as the magnetite content increases, the samples retain their micro-mesoporous character, although the proportion of pores with a diameter of <6 nm decreases slightly (Figures 3, 4). It was assumed that the formation of magnetite particles occurs mainly on the surface of the HPS and in the mouths of the pores, which leads to their blockage and, consequently, a decrease in the specific surface area and a change in the ratio of micro-, meso- and macropores of the samples.

This assumption is confirmed by the results of transmission electron microscopy (Figures 5 and 6). The mean magnetite nanoparticle diameter is  $40 \pm 5$  nm. The mean Ru nanoparticle diameter is  $2.0 \pm 0.5$  nm.

Table 3 shows the results of X-ray photoelectron spectroscopy of catalyst 3 % Ru-Fe<sub>3</sub>O<sub>4</sub>/HPS MN270. XPS data show that the formation of ruthenium nanoparticles occur mainly on the surface of the HPS matrix.

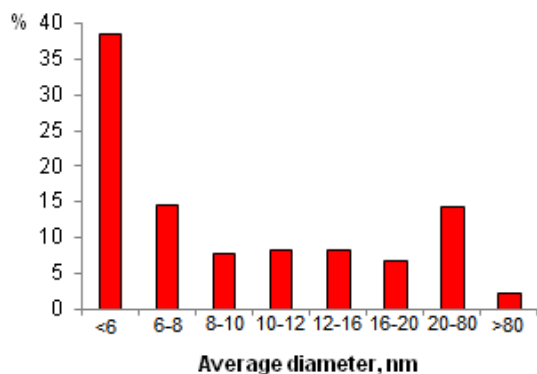


Figure 3: Pore size distributions for HPS MN270.

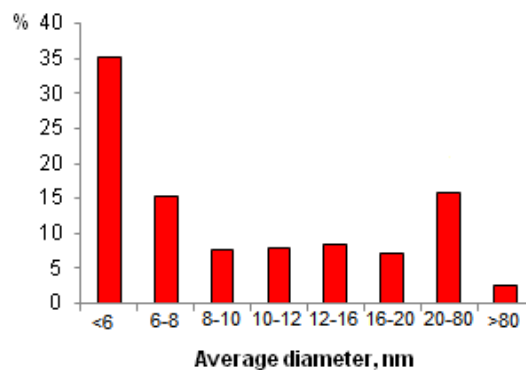


Figure 4: Pore size distributions for 3 % Ru-Fe<sub>3</sub>O<sub>4</sub>/HPS MN270.

The magnetite nature of the magnetic particles was also confirmed by powder X-ray diffraction. The XRD pattern of Fe<sub>3</sub>O<sub>4</sub>/HPS MN270 displays the sharper Bragg reflections whose intensity and positions are typical for those of magnetite (Figure 7).

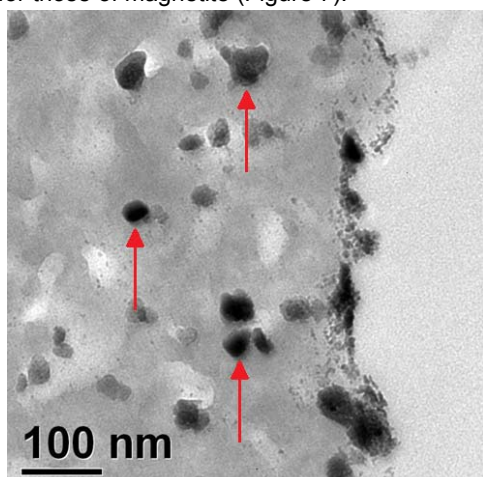


Figure 5: Magnetite nanoparticles with mean diameter  $40 \pm 5$  nm.

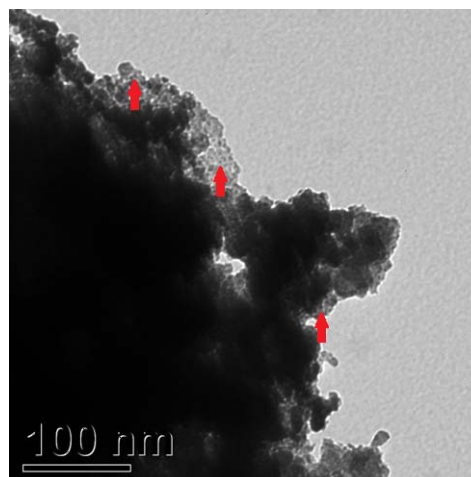


Figure 6: Ru-containing nanoparticles with mean diameter  $2.0 \pm 0.5$  nm.

The 3 % Ru-Fe<sub>3</sub>O<sub>4</sub>/HPS MN270 catalysts synthesized have been studied in the cellulose hydrogenolysis using laboratory setup showing on Figure 8.

Table 3: Surface composition of 3 % Ru-Fe<sub>3</sub>O<sub>4</sub>/HPS MN270 based on XPS data

Element:	%at.	%wt.
C 1s	66.8	45.5
O 1s	25.8	23.5
N 1s	0.2	0.2
Cl 2p	0.4	0.8
Ru 3p <sub>3/2</sub>	3.3	18.9
Fe 2p <sub>3/2</sub>	3.5	11.1

Testing of the catalyst was carried out in the same conditions as in the previous study (Manaenkov et al., 2016<sup>a</sup>): 255 °C, hydrogen partial pressure 60 bar, 50 min, 0.3 g of microcrystalline cellulose (fraction with 0.045-0.063 μm particles size), 0.07 g of 3 % Ru-Fe<sub>3</sub>O<sub>4</sub>/HPS MN270 catalyst, 30 mL of H<sub>2</sub>O, 0.195 mol of Ca(OH)<sub>2</sub> per 1 mol of cellulose. Under said experimental conditions, the maximum selectivity for PG and EG were 20.0 % and 22.6 %, respectively. Cellulose conversion in all runs was 100%.

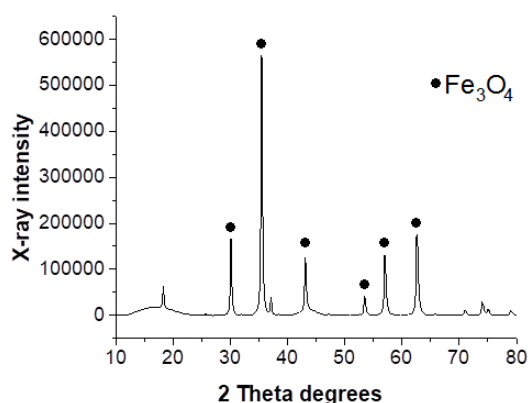


Figure 7: XRD pattern of the  $\text{Fe}_3\text{O}_4/\text{HPS MN270}$ .

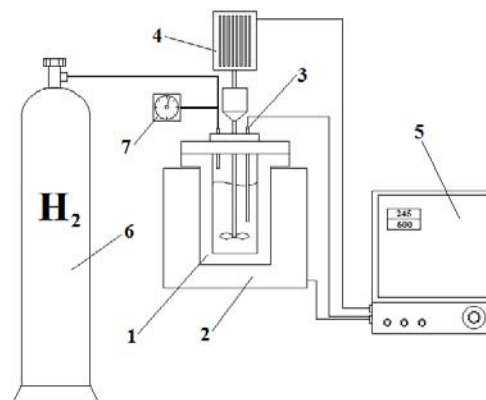


Figure 8: Laboratory setup includes a high-pressure reactor (1), a heater (2), a thermocouple (3), a stirrer motor (4), a control unit (5), a hydrogen bottle (6), and a manometer (7).

Figure 9 presents a typical chromatogram of the liquid phase obtained after the reaction with 3 %  $\text{Ru-Fe}_3\text{O}_4/\text{HPS MN270}$ . The main products of cellulose hydrogenolysis are glycerol, propylene glycol (PG) and ethylene glycol (EG).

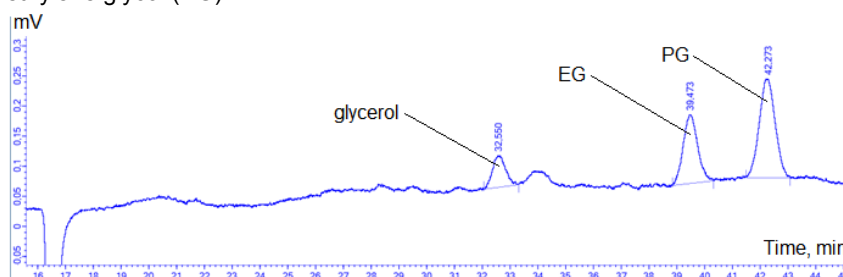


Figure 9: Chromatogram of liquid phase after the reaction (255 °C, 60 bar  $\text{H}_2$ , process duration 55 min, 30 mL water, 0.07 g 3 %  $\text{Ru-Fe}_3\text{O}_4/\text{HPS MN270}$ , 0.3 g cellulose, 0.195 mol of  $\text{Ca}(\text{OH})_2$  per 1 mol of cellulose).

The data in Table 4 show that the selectivity of 3 %  $\text{Ru-Fe}_3\text{O}_4/\text{HPS MN270}$  catalyst was approximately equaled to the selectivity of the magnetically recoverable 5 %  $\text{Ru-Fe}_3\text{O}_4\text{-SiO}_2$  catalyst, which earlier showed good results in the hydrogenolysis of cellulose to glycols (Manaenkov et al., 2016<sup>b</sup>). However, due to the lower percentage of ruthenium in the new catalyst, its specific activity was higher by approximately 35% for EG and 20% for PG (Table 4). To study the catalyst stability, 3 %  $\text{Ru-Fe}_3\text{O}_4/\text{HPS MN270}$  was separated from the reaction medium using a neodymium magnet and then added to a fresh portion of cellulose, distilled water, and  $\text{Ca}(\text{OH})_2$ .

Table 4: Catalytic activities for EG and PG with the catalysts tested

Catalyst	Selectivity, %		Specific catalytic activity calculated as a gram of EG or PG per gram of Ru per hour, $\text{h}^{-1}$	
	EG	PG	EG	PG
3 % $\text{Ru-Fe}_3\text{O}_4/\text{HPS MN270}$	22.6	20.0	39.12	34.62
5 % $\text{Ru-Fe}_3\text{O}_4\text{-SiO}_2$	19.1	20.9	25.29	27.72

255 °C; 60 bar  $\text{H}_2$ ; 55 min; 0.3 g of cellulose; 0.07 g of catalyst; 30 mL  $\text{H}_2\text{O}$ ; 0.195 mol of  $\text{Ca}(\text{OH})_2$  per 1 mol of cellulose.

The data presented in Table 5 indicate that the EG and PG selectivities at 100% conversion (~22.6 and 20 %, respectively) and the activity do not change, revealing that the catalyst is stable under hydrothermal conditions of the hydrogenolysis process. The use of magnetically separable catalysts (MSC) shows many advantages such as convenient separation, efficient recovery, what is especially important with incomplete biomass conversion. According to preliminary estimates, the use of MSC can reduce the cost of the product by 5-10 %, provided that they are stable under hydrothermal conditions for at least 5 cycles.

Table 5: Catalytic activity and selectivity for glycols in the repeated use with 3 % Ru-Fe<sub>3</sub>O<sub>4</sub>/HPS MN270

Catalyst use	Selectivity, %		Specific catalytic activity calculated as a gram of EG or PG per gram of Ru per hour, h <sup>-1</sup>	
	EG	PG	EG	PG
1	22.6	20.0	39.12	34.62
2	22.3	19.7	38.60	34.10
3	22.5	19.6	38.95	33.93

255 °C; 60 bar H<sub>2</sub>; 55 min; 0.3 g of cellulose; 0.07 g of 3 % Ru-Fe<sub>3</sub>O<sub>4</sub>/HPS MN270; 30 mL H<sub>2</sub>O; 0.195 mol of Ca(OH)<sub>2</sub> per 1 mol of cellulose.

#### 4. Conclusions

The synthesis method of catalyst (3 % Ru-Fe<sub>3</sub>O<sub>4</sub>/HPS MN270) was developed. Synthesized magnetically recoverable supports and catalysts were characterized by different physical-chemical methods. The use of this catalyst in the process of microcrystalline cellulose hydrogenolysis in subcritical water at 255 °C, 60 bar hydrogen pressure in 50 minutes allows PG and EG selectivities of 20.0 and 22.6%, respectively, at 100% of cellulose conversion. The catalyst is stable under hydrothermal conditions of the process; it is easily separated from the liquid phase with the external magnetic field and can be reused. Therefore, the results of the research prove the advantages of the use of magnetically retrievable catalysts in biomass processing into chemicals.

#### Acknowledgments

The authors thank L.M. Bronstein from the Nesmeyanov Institute of Organoelement Compounds, RAS. This work was supported by the Russian Foundation for Basic Research, project nos. 18-08-00404, 18-29-06004, 19-08-00414; and by the Russian Science Foundation, project no. 18-19-00240.

#### References

- Luo C., Wang S., Liu H., 2007, Cellulose conversion into polyols catalyzed by reversibly formed acids and supported ruthenium clusters in hot water. *Angew. Chem. Int. Ed.* 46, 7636-7639.
- Manaenkov O., Matveeva V., Sinitzyna P., Ratkevich E., Kislitza O., Doluda V., Sulman E., Sidorov A., Mann J., Losovyj Y., Bronstein L., 2016a, Magnetically Recoverable Catalysts for Cellulose Conversion into Glycols. *Chemical Engineering Transactions*, 52, 637-642.
- Manaenkov O., Mann J., Kislitza O., Losovyj Y., Stein B., Morgan D., Pink M., Lependina O., Shifrina Z., Matveeva V., Sulman E., Bronstein L., 2016b, Ru-containing Magnetically Recoverable Catalysts: A Sustainable Pathway from Cellulose to Ethylene and Propylene Glycols. *ACS Appl. Mater. Interfaces*, 8, 21285-21293.
- Podolean I., Negoai A., Candu N., Tudorache M., Parvulescu V. I., Coman S. M., 2014, Cellulose Capitalization to Bio-chemicals in the Presence of Magnetic Nanoparticle Catalysts. *Top. Catal.* 57(17-20), 1463-1469.
- Sidorov S.N., Bronstein L.M., Davankov V.A., Tsyurupa M.P., Solodovnikov S.P., Valetsky P.M., Wilder E.A., Spontak R.J., 1999, Cobalt Nanoparticle Formation in the Pores of Hyper-Cross-Linked Polystyrene: Control of Nanoparticle Growth and Morphology. *Chem. Mater.*, 11, 3210-3215.
- Sugiyama S., Tanaka H., Bando T., Nakagawa K., Sotowa K.-I., Katou Y., Mori T., Yasukawa T., Ninomiya W., 2013, Liquid-phase oxidation of propylene glycol using heavy-metal-free Pd/C under pressurized oxygen. *Catal. Today*, 203, 116-121.
- Tsvetkova I.B., Matveeva V.G., Doluda V.Y., Bykov A.V., Sidorov A.I., Schennikov S.V., Sulman M.G., Valetsky P.M., Stein B.D., Chen C.-H., 2012, Pd(II) Nanoparticles in Porous Polystyrene: Factors Influencing the Nanoparticle Size and Catalytic Properties. *J. Mater. Chem.*, 22, 6441-6448.
- Wang D., Astruc D., 2014a, Fast-Growing Field of Magnetically Recyclable Nanocatalysts. *Chem. Rev.* 114, 6949-6985.
- Wang D., Astruc D., 2014b, Magnetically recoverable ruthenium catalysts in organic synthesis. *Molecules*, 19(4), 4635-4653.
- Yue H., Zhao Y., Ma X., Gong J., 2012, Ethylene glycol: properties, synthesis, and applications. *Crit. Rev.: Chem. S. Rev.* 41, 4218-4244.
- Zhang J., Wu S., Liu Y., 2014, Direct conversion of cellulose into sorbitol over a magnetic catalyst in an extremely low concentration acid system. *Energy Fuels*. 28, 4242-4246.